

Study on stiffness deterioration in steel-concrete composite beams under fatigue loading

Bing Wang^{1a}, Qiao Huang^{2b}, Xiaoling Liu^{*3} and Yong Ding^{1c}

¹School of Civil and Environmental Engineering, Ningbo University, Ningbo 315211, China

²School of Transportation, Southeast University, Nanjing 210096, China

³Faculty of Maritime and Transportation, Ningbo University, Ningbo 315211, China

(Received July 29, 2019, Revised October 16, 2019, Accepted October 21, 2019)

Abstract. The purpose of this paper is to investigate the degradation law of stiffness of steel-concrete composite beams after certain fatigue loads. First, six test beams with stud connectors were designed and fabricated for static and fatigue tests. The resultant failure modes under different fatigue loading cycles were compared. And an analysis was performed for the variations in the load-deflection curves, residual deflections and relative slips of the composite beams during fatigue loading. Then, the correlations among the stiffness degradation of each test beam, the residual deflection and relative slip growth during the fatigue test were investigated, in order to clarify the primary reasons for the stiffness degradation of the composite beams. Finally, based on the stiffness degradation function under fatigue loading, a calculation model for the residual stiffness of composite beams in response to fatigue loading cycles was established by parameter fitting. The results show that the stiffness of composite beams undergoes irreversible degradation under fatigue loading. And stiffness degradation is associated with the macrobehavior of material fatigue damage and shear connection degradation. In addition, the stiffness degradation of the composite beams exhibit S-shaped monotonic decreasing trends with fatigue cycles. The general agreement between the calculation model and experiment shows good applicability of the proposed model for specific beam size and fatigue load parameters. Moreover, the research results provide a method for establishing a stiffness degradation model for composite beams after fatigue loading.

Keywords: steel-concrete composite beam; fatigue; stiffness degradation; relative slip; bridge

1. Introduction

Steel-concrete composite beams have been widely used in bridges and building structures because they make full use of the mechanical properties of the two materials (Zhou *et al.* 2018, Chen and Sudibyo 2019, Zhou *et al.* 2016 and Foraboschi 2014). However, under long-term traffic loading, fatigue damage occurs in composite bridges, which seriously endangers their safety and durability (Deng *et al.* 2019, Runnian and Demin 2013 and Foraboschi 2016b). Usually, fatigue damage in a structure will accumulate and increase with loading cycles, which leads to the deterioration of the stiffness and bearing capacity of the structure. Once a sufficiently accumulating damage produces an unpredictable failure an unpredictable failure, which can cause heavy casualties or property losses (Kwon and Dan 2010 and ADASOORIYA *et al.* 2014). Therefore, it is particularly important to determine the law of damage

accumulation and performance degradation of composite beams under fatigue loading, which can be used to suppress the fatigue degradation of composite beams by controlling the mechanical properties of the beams.

The stiffness of composite beams is an important indicator that reflects the fatigue degradation of composite beams, and it is easy and simple to perform stiffness tests. Exploring the residual stiffness degradation law of composite beams under fatigue loads is of great significance to predict the performance of composite beams at different stages of service. To date, many scholars have carried out extensive experimental studies on the fatigue behavior of composite beams (Hanswille *et al.* 2007, Wang *et al.* 2017, Lin *et al.* 2016 and Sjaarda *et al.* 2017). Some experimental results have shown the stiffness degradation of composite beams under fatigue loads. For example, Song *et al.* (2018) studied the residual deflection behavior of steel-concrete composite beams under a negative bending moment, and found that both the relative slip between the steel beam and concrete flange and the residual deflection increases gradually with increases in the number of loading cycles.

Yang *et al.* (2016) performed fatigue tests of steel-precast concrete slab composite beams and showed a substantial stiffness degradation of composite beams under fatigue loading. The additional mid-span deflection of composite beams caused by fatigue is approximately 45.1% of the initial deflection. Hanswille and Porsch (2014) concluded that the initial stiffness of composite beams

*Corresponding author, Ph.D.

E-mail: liuxiaolingseu@163.com

^a Ph.D.

E-mail: wangbing050114@163.com

^b Professor

E-mail: qhuanghit@126.com

^c Professor

E-mail: dingyong@nbu.edu.cn

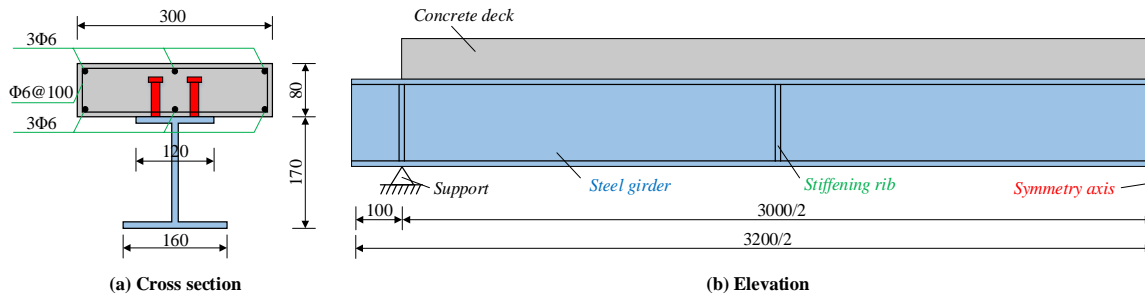


Fig. 1 The size and construction of composite beam specimens (Unit: mm)

decreased by approximately 18.2% after 1.37 million fatigue loading cycles.

The above-mentioned studies were limited to describing the phenomenon of stiffness degradation. In contrast, research regarding the stiffness degradation law of composite beams is still insufficient, and there is still no suitable calculation model to determine the stiffness change in composite beams under fatigue loading.

Therefore, on the basis of previous studies, we selected steel-concrete composite beams with stud connectors, which are the most widely used composite beams, and conducted static and fatigue tests on six test beams. Subsequently, characteristics of stiffness variation in composite beams and the main related factors under different fatigue loading conditions were analyzed. Then, based on the stiffness degradation function model, a calculation model for the residual stiffness of composite beams with respect to the number of fatigue loading cycles was established and verified by parameter fitting. In this study, a new method was established for calculation in stiffness degradation of composite beams under fatigue loading.

2. Experimental design

2.1 Specimen size

The test beams were designed according to the following sizes and reinforcements. The length of the steel beam and the concrete flange plate are respectively 3.2 m and 3.0 m. The calculated span is 3.0 m. The steel beam is welded by Q345 with a thickness of 10 mm. The width of the upper flange plate is 120 mm, and the width of the lower flange plate is 160 mm. The depth of the web plate is 150 mm. The concrete flange plate is made of C50 concrete and has a width of 300 mm and a thickness of 80 mm. To improve the local stability of the steel girders, vertical stiffeners were installed at the bearings, quarter-span and mid-span positions. The shear connectors in the test composite beams are assumed to be fully connected (Hu and Zhao 2013 and Yatim *et al.* 2013), i.e., the degree of shear connection is 1.0. The studs with material of ML-15 were 13 mm in diameter and 60 mm in length, which met the requirements of the code. The studs were arranged in double rows with 60 mm transverse spacing and 215 mm longitudinal spacing. The size and construction of the composite beam specimens are shown in Fig. 1.

2.2 Test loading mode

The test was performed on a multifunctional structure testing system (JAW-500K) equipped with an electrohydraulic servo actuator. The system provides a measurement range of 500 kN for low-friction spherical hinges and can be used for static and dynamic loading.

The test beam had a simply supported boundary condition, and single-point loading was adopted at the mid-span, as shown in Fig. 2. To understand the stiffness degradation law of the test beams under fatigue loads, three groups of loading condition were employed. The first group involves a static loading failure test for one specimen, designated as SCB-1. The purpose is of this first group is to determine the static ultimate bearing capacity of the test beams (P_u). The second group involves a complete fatigue test for one specimen, designated as FCB-1. The result of the second group is used to determine the fatigue life of the test beams (N). The third group involves an incomplete fatigue failure test, namely a static loading failure test after a certain number of fatigue cycles. The four specimens in the third group, designated SFCP-1, SFCP-2, SFCP-3 and SFCP-4, are subjected to static failure tests after 0.5, 1, 1.5 and 2 million fatigue loading cycles, respectively. The specific parameters of fatigue loading are shown in Table 1. Besides, fatigue loading was applied by a sine wave with a loading frequency of 4 Hz. The control mode was force control.

It should be noted that the fatigue stress amplitude of the lower steel beam edge at the mid-span of the composite beam is mainly used as the fatigue loading control during the design process of this test. According to the fatigue details of the welded section of the steel I-beam in Eurocode 4: Design of Composite Structures (BSI 2005), the stress amplitude of the lower edge of the steel beam corresponding to fatigue life of 2 million cycles is 100 MPa, and the ratio of the fatigue loading amplitude in this test is $0.25P_u$.

During the loading process, the load value can be obtained from the internal load cell. The displacement measurement includes several pieces of information, such as the deflection of the test beam at the mid-span and quarter-span, the relative slip of the half span at the interface between the steel beam and the concrete flange plate, as shown in Fig. 3.



Fig. 2 The loading process of the test beam and the testing system

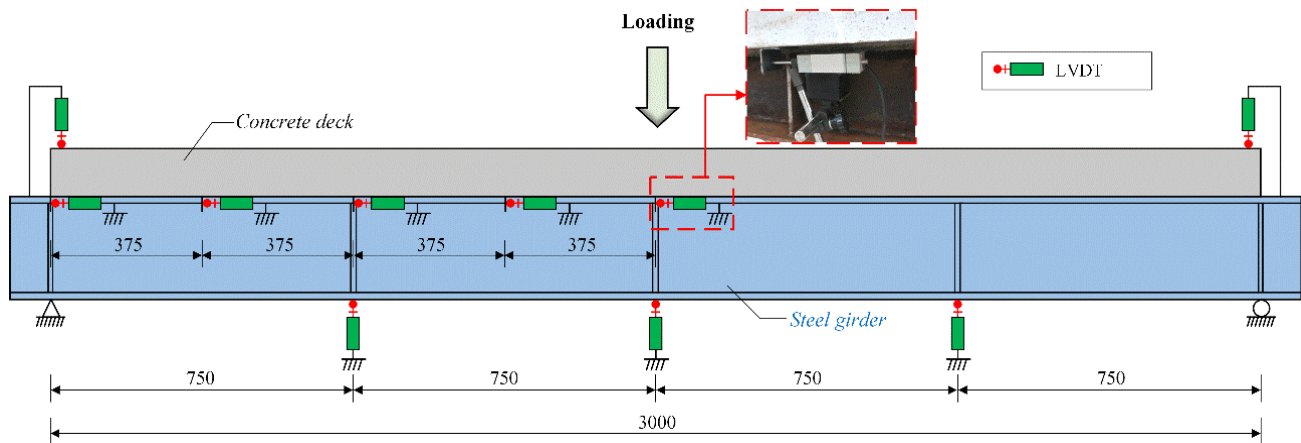


Fig. 3 Measuring-point layout of the specimen (units are in mm)

Table 1 Fatigue modes and test results of test beams

Specimens	Test mode	Fatigue parameter			P_s (kN)	Failure mode
		P_{max}/P_u	P_{min}/P_u	$n(\times 10^6)$		
SCB-1	Static load failure test	-	-	-	228	Concrete crush
FCB-1	Complete fatigue test	0.60	0.35	2.076	/	Stud failure
SFCB-1	Incomplete fatigue failure test	0.60	0.35	0.5	225	Concrete crush
SFCB-2	Incomplete fatigue failure test	0.60	0.35	1.0	213	Stud failure
SFCB-3	Incomplete fatigue failure test	0.60	0.35	1.5	200	Stud failure
SFCB-4	Incomplete fatigue failure test	0.60	0.35	2.0	158	Stud failure

Note: P_{max} is the upper limit of the fatigue loading of the test beams; P_{min} is the lower limit of the fatigue loading of the test beams; and P_s is the residual bearing capacity of the test beams after fatigue loading



Fig. 4 Failure mode of test beams

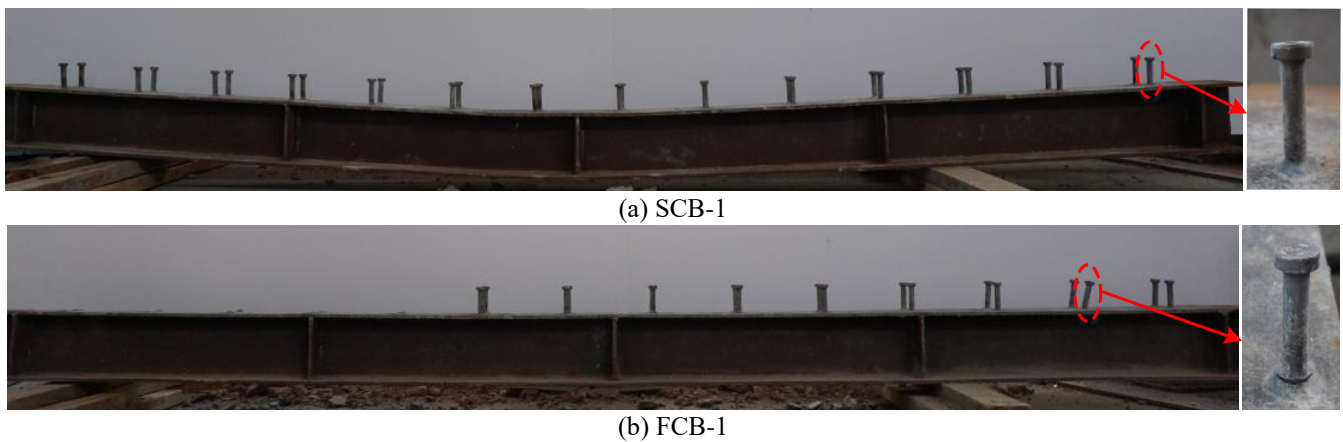


Fig. 5 Static and fatigue failure modes of the studs in the test beam

3. Test results and discussions

3.1 Failure modes

There are two typical failure modes of the test beams according to testing results. The failure mode of the test beam in the static load failure test (SCB-1) is a combination of the steel beam yielding and the concrete crushing at the mid-span, as shown in Fig. 4 (a). In contrast, the test beam in the complete fatigue failure test (FCB-1) failed because the stud sheared off, which caused disengagement between the steel beam and concrete slab, as shown in Fig. 4 (b).

To further compare the static and fatigue failure modes of the studs in the test beam, the concrete of test beams SCB-1 and FCB-1 was chiseled off. As exhibited in Fig. 5(a) and (b). It can be found that the stud connectors still remained intact under static damage, while the studs on one side of the test beam had been cut off under complete fatigue test. It proved that the fatigue loading could cause failure of the studs inside the concrete plate, which could in turn lead to fatigue damage.

Table 1 gives the failure modes of each test beam in the three test groups. The failure modes of the test beams are mainly affected by the number of loading cycles. When the number of loading cycles is small, such as SFCB-1 tests, the failure modes after fatigue testing are featured with the

yielding of steel beams and the crushing of concrete in the mid-span, similar to those of the static tests. When the number of loading cycles is large, such as SFCB-2~SFCB-4 tests, all of the failure modes are involved the stud shearing off. These results show that under fatigue load, the bearing capacities of stud connectors deteriorate, which causes the connection degree of composite beams to transition from complete shear connection to partial shear connection and the failure mode to transition from concrete crushing at the mid-span to stud shear failure. The decrease in the shear connection degree of composite beams is also an important reason for the overall stiffness drop of composite beams.

3.2 Analysis of experimental results

3.2.1 Stiffness expression of composite beam

According to the basic theory of material mechanics, the mid-span deflection f of a beam under a certain load can be expressed as

$$f = \alpha \frac{ML^2}{B} \quad (1)$$

where α is the deflection coefficient of the beam, dependent on structural support and loading form. In some literature, α is obtained by fitting specific experimental data (Gao and

Zhang 2013 and Zhu *et al.* 2014); M is the maximum bending moment of the mid-span section of the beam; L is the calculated span of the beam; and B is the flexural rigidity of the beam, and can be expressed as $B=EI_0$, where E is the elastic modulus of the beam and I_0 is the inertia moment of the beam section.

For convenience of calculation, the area of concrete flange on composite section is converted into equivalent steel section. It can be considered that the composite section is made of a homogeneous material, and the simple supporting condition is assumed for composite beam. Consequently, $\alpha=1/12$ is obtained by derivation. Then the expression of bending stiffness B of composite beams can be obtained by inverse calculation of formula (1).

$$B = \frac{ML^2}{12f} \quad (2)$$

In this test, the bearing condition of the test beam is simple, and the loading mode at the mid-span is single-point loading. In the fatigue loading process, when a certain number of cycles n is performed, the machine is stopped and unloaded, and a static test is performed. The load increases from 0 to the upper limit of fatigue load P_{max} . In such case, the mid-span deflection of the test beam is recorded as f_n , so The composite beam stiffness B_n after n -fatigue loading is written as

$$B_n = \frac{PL^3}{48f_n} \quad (3)$$

where P here corresponds to the upper limit of fatigue load $P_{max} = 0.6P_u = 136$ kN; f_n is the deflection at the upper limit of fatigue loading.

3.2.2 Test results analysis of composite beams

(1) Load-deflection curves

The load-deflection curve is an important index that reflects the overall performance of composite beams (Esendemir 2006). Moreover, load-deflection curves can also reflect the characteristic changes in a series of parameters, such as stiffness, bearing capacity and ductility of composite beams. Fig. 6 shows the mid-span load-deflection curves of the static failure test beams and the static failure test beams after different numbers of fatigue loading cycles. It can be seen from the figure that the number of fatigue loading cycles has a more substantial effect on the test beam. With the increase in the number of cyclic loadings, the bearing capacity of the test beam decreases, the stiffness in the linear elastic stage decreases, and the ductility decreases.

To further compare the residual stiffness degradation of different test beams after different numbers of fatigue loading cycles, the residual stiffness of the test beams SCB-1 and SFCB-1~SFCB-4 after different cycles of fatigue cycles was calculated by Eq. (4), as shown in Fig. 7.

As shown in Fig. 7, the residual static stiffness of the test beam tends to decrease with increasing fatigue loading cycles. For example, the residual stiffness of test beam SFCB-4 after 2 million fatigue loading cycles decreases by 26.7% compared with that of SCB-1. However, it should be

noted here that the stiffness of SFCB-1 after 500,000 fatigue loading cycles increases by 1.8% compared with SCB-1. This phenomenon may be due to the smaller number of fatigue loading cycles in the specimens, which could result in other influencing factors including equipment measurement error, specimen processing error, and material inhomogeneity masking substantial decreases in the stiffness of SFCB-1 beam.

(2) Residual deflection

Residual deflection is the directly correlated with stiffness degradation in the test beams. Residual deflection reflects the damage development in the test beams and can even be used to predict the damage of test beams (Huang *et al.* 2019 and Liu *et al.* 2018). In the process of fatigue loading, a static test was performed after a certain number of cycles, and the change in the residual deflection of the test beam was recorded in these instances. Fig. 8 shows the growth curve of the residual deflection in the test beam with increasing numbers of cyclic loadings.

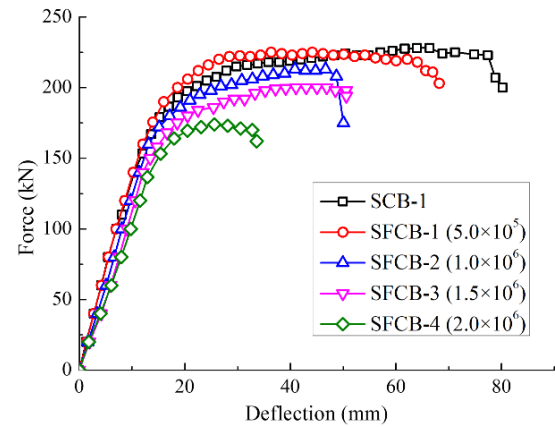


Fig. 6 Mid-span load-deflection curves

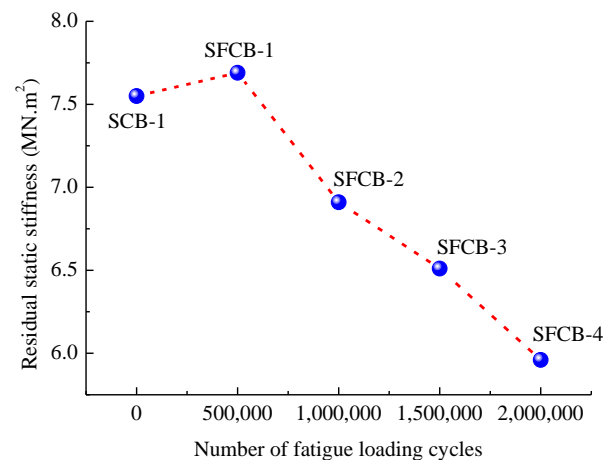


Fig. 7 Residual static stiffness after cyclic fatigue loading

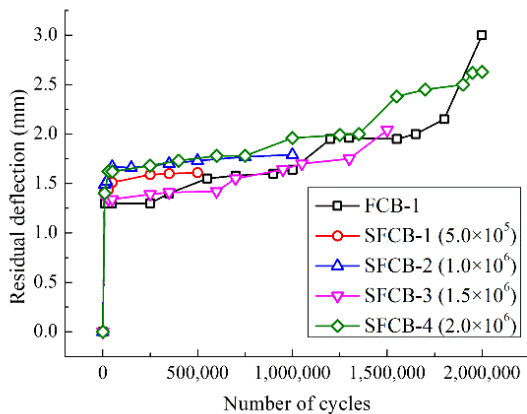


Fig. 8 Residual mid-span deflection growth curves

As shown in Fig. 8, the growth law of residual deflection in the test beams can be roughly divided into three stages: 1) In the initial stage of cyclic loading, the residual deflection increases rapidly, and the value of each test beam reaches approximately 1.5 mm. The main reason for this increase in residual deflection is that the contact between the concrete flange plate and studs is not compact, and there is elastic compression in the concrete flange plate. 2) In the middle stage of cyclic loading, the residual deflection of the test beam increases steadily and slowly, and it continues this trend for a long time. 3) In the third stage of cyclic loading, especially when it approaches the fatigue life of the test beam, the growth rate of the residual deflection increases again. Test beams SFCB-1~SFCB-3 exhibit only the first two stages because they are subjected to a relatively small number of loading cycles and are thus far from reaching their fatigue life.

(3) Relative slip

Relative slip occurs at the interface of the composite beam during fatigue loading. Relative slip is directly related to whether concrete flanges can work well with steel beams and is also a major factor affecting the overall stiffness of beams (Focacci *et al.* 2015 and Girhammar 2009).

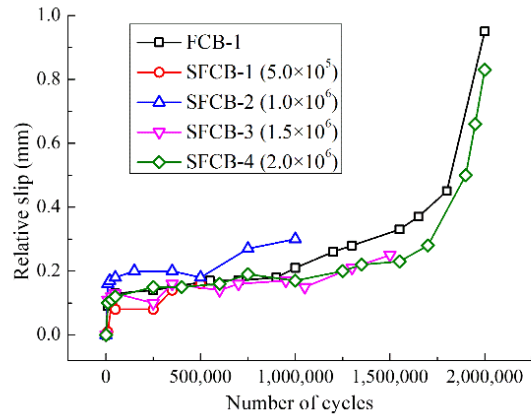


Fig. 9 Relative slip growth curves of the test beam

Fig. 9 shows the growth curve of the relative slip at the end of the test beam in response to the number of cyclic loadings. The relative slip growth curves of the composite beams generally presents a three-stage growth trend, similar to the residual deflection curves.

(4) Stiffness degradation in the fatigue process

To further analyze the stiffness degradation of test beams under fatigue loading, the stiffness values of composite beams corresponding to FCB-1 and SFCB-1~SFCB-4 under different number of fatigue loading cycles were calculated by equation (2); these values are shown in Fig. 10.

It can be seen from Fig. 10 that the bending stiffness of the test beams exhibit different degrees of decline in response to increases in the number of cyclic loadings, and they exhibit a monotonic S-shaped decreasing trend. The stiffness degradation ranges of test beams FCB-1 and SFCB-4 are 23.8% and 26.2%, respectively, after 2 million fatigue loading cycles, and the degradation degree is obvious. In addition, the initial stiffness of the five test beams is about 8 MN.m². The maximum error is kept within 6% despite the errors during fabrication and testing.

Furthermore, the correlation among the stiffness degradation in each test beam, the residual deflection and relative slip growth (presented in the previous section) is analyzed. The results of this analysis are listed in Table 2.

Table 2 Correlation analysis of the stiffness, residual deflection and relative slip values of the test beams

Test beam number	Number of loading cycles / $\times 10^6$	Influencing factors	
		Residual deflection	Relative slip
FCB-1	2.0756	-0.92	-0.86
SFCB-1	0.5	-0.18	-0.70
SFCB-2	1.0	-0.76	-0.94
SFCB-3	1.5	-0.61	-0.76
SFCB-4	2.0	-0.84	-0.88

Table 2 indicates a strong negative correlation of the stiffness of the test beams with both the residual deflection and relative slip, especially for the test beams subjected to a higher number of fatigue loading cycles, such as FCB-1 and SFCB-4. Their correlation coefficients are always less than -0.8 with a minimum of -0.92, implying the intimacy of negative correlation. The increase in residual deflection reveals the fatigue damage in composite beams, which includes the material damage of steel beams, concrete and stud connectors. The increase in the relative slip mainly reflects the weakening of the shear connection degree of the composite beams. Therefore, there are many factors that affect the overall stiffness degradation of composite beams under fatigue loading. In fact, stiffness degradation is the macroscopic performance of material fatigue damage and shear connection degradation.

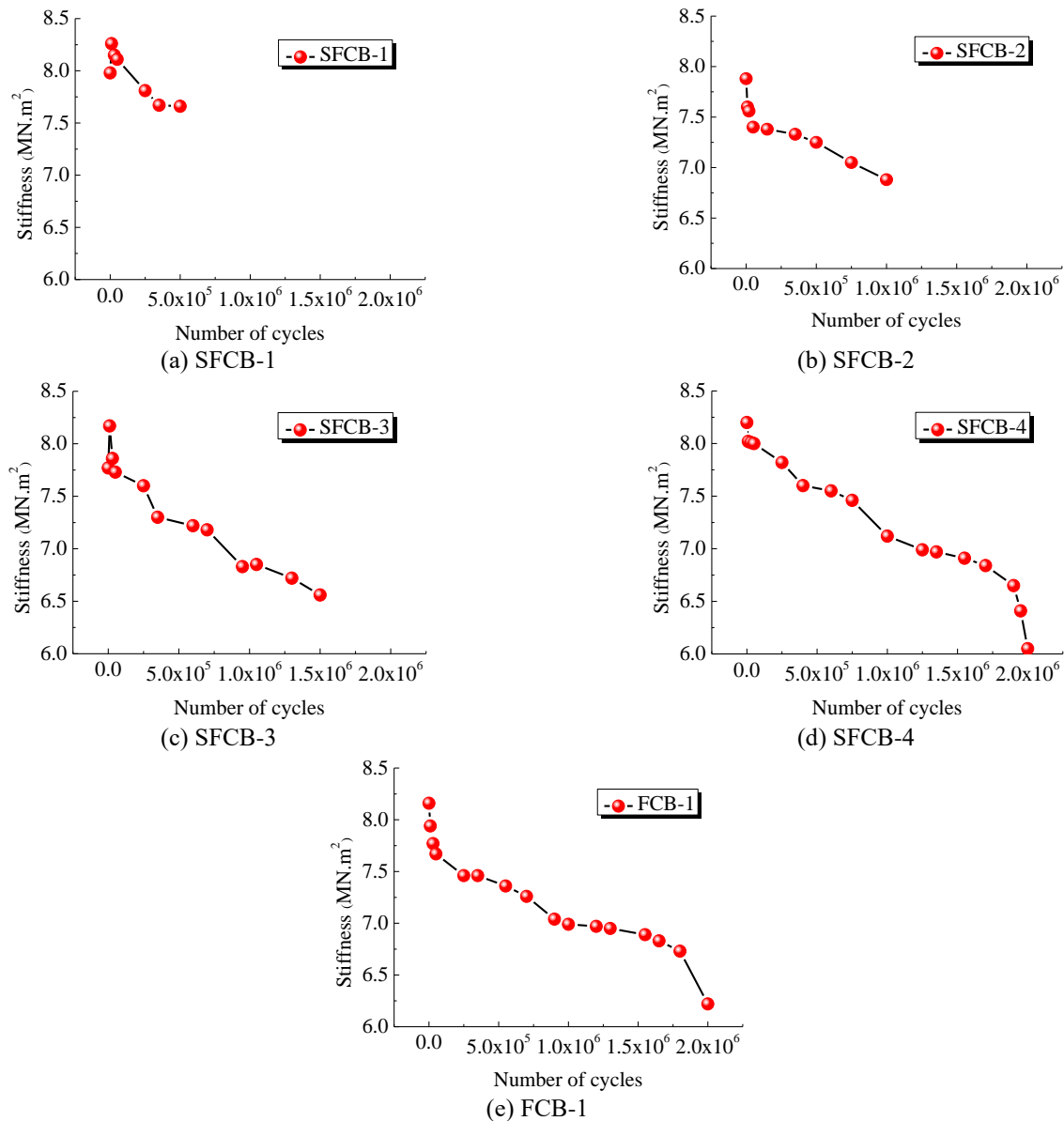


Fig. 10 Residual stiffness variations in SFCB-1~SFCB-4 and FCB-1

4. Stiffness degradation law of composite beams under fatigue loading

4.1 Characterization of the Residual Stiffness Degradation of Composite Beams

From previous analysis, it can be seen that the stiffness degradation in composite beams after cyclic fatigue loading, as a macroscopic manifestation, is associated with the overall fatigue damage in the composite beams. Based on the mesoscopic perspective, this degradation is caused by the damage of concrete, steel beams, and stud connectors. Relevant research shows that the definition of damage due to fatigue refers to slow but persistent propagation of crack until reaching the critical length (Foraboschi 2016). That phenomenon involves each connected element (e.g., steel and concrete beams) as well as the connector (e.g., the stud

shear connector). Fatigue, the microscopic slow crack propagation, is a delayed debonding of fracture mechanics. Actually, the relative slip growth curves of the test beam shown in Fig. 9 could be explained by such phenomenon.

However, it is often difficult to quantify the meso-damage of structures directly, and the damage relationship between materials is also very complex. Therefore, in the present paper the composite beams are simplified as a single and individual component, and changes in the overall stiffness of the beams are used to characterize directly the gross fatigue damage degree of composite beams.

The degree of fatigue damage characterized by the overall stiffness degradation of the composite beam is calculated as

$$D = \frac{B_0 - B_n}{B_0 - B_N} \quad (4)$$

where, D is the degree of fatigue damage, $D \in [0,1]$; B_0 is the initial stiffness of the composite beam; B_n is the stiffness of the composite beam subjected to n times of fatigue loading; B_N is the stiffness of the composite beam under fatigue failure.

Assuming the composite beam stiffness damage changes according to a function of the fatigue life ratio, expressed as $\zeta(n/N)$ related to, the following equation could be derived.

$$D = \frac{B_0 - B_n}{B_0 - B_N} = \zeta\left(\frac{n}{N}\right) \quad (5)$$

Hence, the real-time stiffness B_n of a composite beam under n cyclic loading can be obtained.

$$B_n = B_0 - (B_0 - B_N) \zeta\left(\frac{n}{N}\right) \quad (6)$$

The parameters B_0 and B_N can be obtained by calculating the deflection measured by the experiments, which means that the most important thing is the determination of the stiffness degradation function $\zeta(n/N)$.

4.2 Stiffness degradation function

According to previous literatures (Amiri *et al.* 2017 and Yan *et al.* 2016), the stiffness degradation function generally exhibits the following features:

(a) A composite beam has no damage before fatigue loading. Namely when $n/N=0$, $\zeta(n/N)=0$. Therefore, the stiffness of the composite beam is equal to its initial stiffness B_0 .

(b) When fatigue failure occurs, the damage in a composite beam reaches a maximum and $n/N=1$. Moreover, when $\zeta(n/N)=1$, the stiffness of a composite beam decreases to B_N .

(c) The degradation trend of a composite beam presents a common feature of clearly S-shape. This means that the degradation of a composite beam is linearly stable in the middle stage and decreases sharply at the beginning and end of loading.

Functions satisfying the above rules (a) and (b) are relatively simple to construct, but rule (c) is relatively strict. After many attempts and referring to the functions adopted in references (Cheng 2011), functions satisfying the above requirements are preliminarily constructed as follows

$$\zeta\left(\frac{n}{N}\right) = 1 - \frac{1 - \left(\frac{n}{N}\right)^u}{\left(1 - \frac{n}{N}\right)^v} \quad (7)$$

where, u and v are the parameters to be determined.

By substituting formula (7) into formula (6), a formula for calculating stiffness degradation in composite beams with respect to the number of cyclic loadings n can be calculated as

$$B_n = B_0 - (B_0 - B_N) \left[1 - \frac{1 - \left(\frac{n}{N}\right)^u}{\left(1 - \frac{n}{N}\right)^v} \right] \quad (8)$$

It is found that any type of stiffness degradation law can be described by changing the values of u and v . The initial degradation rate in the stiffness degradation curve is determined by parameter u , whereas the degradation rate near failure is determined by parameter v . The values of u and v can be obtained by binary parameter fitting with experimental values.

4.3 Establishment and verification of the stiffness degradation model for composite beams

In the five test beams tested in this paper, only FCB-1 experienced fatigue failure, and its fatigue life was 20,756,000 cyclic loadings. Data fitting for the stiffness degradation is performed according to formula (5). The initial stiffness B_0 is 8.16 MN.m², and B_N is the critical stiffness for fatigue failure. However, fatigue failure occurred instantaneously in the test. Therefore, it was impossible to obtain the value directly. In this paper, the stiffness value measured at the last cyclic loading (2 million times) before failure is chosen as the value of B_N (6.22 MN.m²).

Fig. 11 is the fitting result of stiffness degradation for test beam FCB-1. The goodness of fit R^2 is 0.959.

The figure shows that the stiffness of the test beam decreases rapidly in the initial and final stages of fatigue loading. In the middle stage of loading, the stiffness decreases relatively slowly, and the stiffness degradation exhibits an obvious S-shaped tendency. By substituting the fitted parameters u and v into formula (8), the stiffness degradation formula for composite beams is obtained as follows

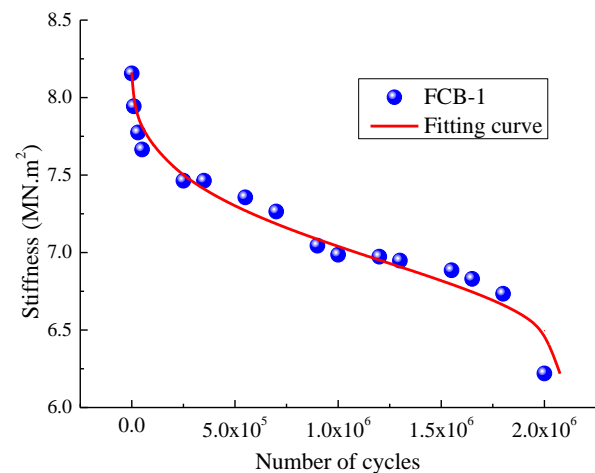


Fig. 11 Stiffness deterioration fitting curve of the FCB-1 test beam

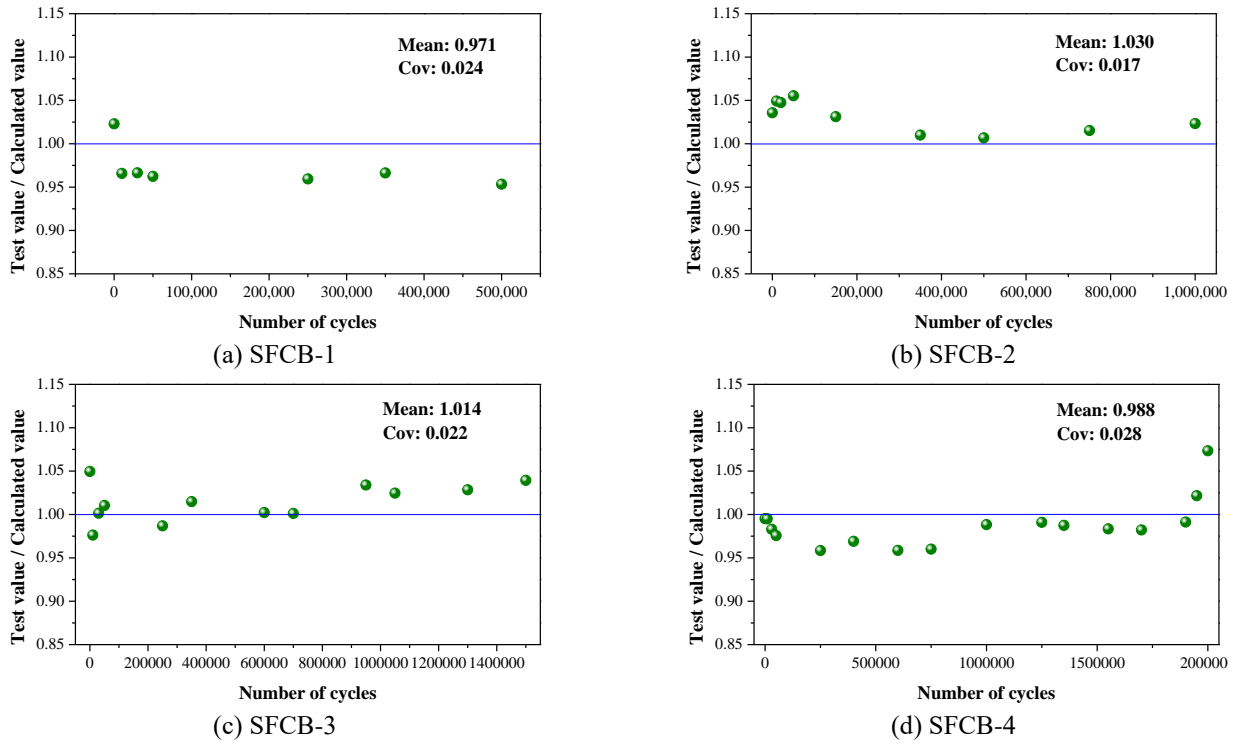


Fig. 12 Comparison of stiffness experimental values and calculated values of SFCB-1~SFCB-4

$$B_n = B_0 - (B_0 - B_N) \left[1 - \frac{1 - \left(\frac{n}{N}\right)^{0.439}}{\left(1 - \frac{n}{N}\right)^{0.657}} \right] \quad (9)$$

where $B_0=8.16 \text{ MN.m}^2$ and $B_N=6.22 \text{ MN.m}^2$.

To verify the validity of formula (9), the calculated results were compared with the experimental results of SFCB-1-4, as shown in Fig. 12. The results show that the experimental values of the four test beams are in good agreement with the calculated values of formula (9). The average fatigue life ratios of the two beams are between 0.971 and 1.014, and the coefficients of variation are between 0.022 and 0.028. It can be seen that the stiffness degradation formula proposed in this paper has certain applicability for the same batch of test beams with the same fatigue loading modes.

4.4 Discussion

According to the research results of the stiffness degradation method and stiffness degradation calculation formula of composite beams in this paper, the deformation and fatigue degradation and damage of steel-concrete composite beams subjected to fatigue loading can be assessed and predicted.

The stiffness degradation method of composite beams proposed in this paper only provides an idea and approach for establishing the stiffness degradation model for composite beams under fatigue loading. When there are a group of composite beams, the stiffness degradation

formula of these composite beams can be obtained by fitting the data from only a few (one or several) composite beams. However, since the initial stiffness of a composite beam is mainly affected by its cross-sectional characteristics, its final stiffness is affected not only by geometric size but also by the fatigue loading parameters. Therefore, when the size and fatigue loading parameters of composite beams are different, the stiffness degradation formula established in this paper is no longer applicable. However, a stiffness degradation model can still be obtained by fitting the relevant parameters of formula (8) with the measured data.

In addition, to reduce the fatigue stiffness degradation of steel-concrete composite girder bridges in practical engineering applications, it is suggested that the stiffness degradation effect be accounted for in the design process of composite girder bridges, and technical measures such as improving the shear connection degree of composite girders and increasing the safety factor of composite girder structures can be adopted.

5. Conclusions

In this paper, residual stiffness and stiffness degradation model of composite beams were investigated. Static and fatigue tests of six test beams were performed. Variation in stiffness in composite beams and the potential factors under different fatigue loading conditions were analyzed. Based on the stiffness degradation function model, a calculation model for the residual stiffness of composite beams with respect to the number of fatigue loading cycles was

established and verified by parameter fitting. The following conclusions are obtained:

- The stiffness of steel-concrete composite beams could gradually and irreversibly degenerate under fatigue loading, and there are many factors affecting the stiffness degradation. In fact, stiffness degradation is the macroscopic manifestation of material fatigue damage and shear connection degradation.

- According to fatigue test results, the stiffness degradation law of steel-concrete composite beams presents monotonic S-shaped decreasing curves. The maximum stiffness degradation range of the test beams after 2 million fatigue loading cycles is 26.2%, which is substantial.

- The theoretical formula for calculating the stiffness degradation of steel-concrete beams is obtained by fitting the measured stiffness data and constructing a function consistent with the stiffness degradation response of composite beams. The formula can quantitatively describe the stiffness degradation.

- In the case of different beam size and fatigue load parameters, the stiffness degradation formula established in this paper is no longer applicable. However, it provides an idea and approach for evaluating the stiffness degradation for composite beams under fatigue loading. In the design of composite beams, technical measures such as improving the shear connection degree and increasing the safety factor of composite beams can be utilized to reduce the fatigue stiffness degradation.

Acknowledgments

The research described in this paper was financially supported by the Natural Science Foundation of Zhejiang Province (No.LQ19E080006) and National Natural Science Foundation of China (No. 51808301). This work was also sponsored by Fund of National Engineering and Research Center for Mountainous Highways (No.GSGZJ-2019-04).

References

- Adasooriya, N.D. and Siriwardane, S.C. (2014), "Remaining fatigue life estimation of corroded bridge members", *Fatigue Fract. Eng. Mater. Struct.*, **37**(6), 603-622. <https://doi.org/10.1111/ffe.12144>.
- Amiri, A., Cavalli, M.N. and Ulven, C.A. (2017), "A new approach of stiffness degradation modeling for carbon fiber-reinforced polymers under cyclic fully reversed bending", *J. Compos. Mater.*, **51**(20), 2889-2897. <https://doi.org/10.1177/0021998317690239>.
- British Standards Institution (2005), Eurocode 4: Design of Composite Structures – Part 1.2 General rules and rules for bridges, BS EN 1994-1-2, BSI, London, UK.
- Chen, C.C., and Sudibyo, T. (2019), "Behavior of partially concrete encased steel beams under cyclic loading", *Int. J. Steel Struct.*, **19**(1), 255-268. <https://doi.org/10.1007/s13296-018-0114-y>.
- Cheng, L. (2011), "Flexural fatigue analysis of a CFRP form reinforced concrete bridge deck", *Compos. Struct.*, **93**(11), 2895-2902. <https://doi.org/10.1016/j.compstruct.2011.05.014>.
- Deng, W., Xiong, Y., Liu, D. and Zhang, J. (2019), "Static and

- fatigue behavior of shear connectors for a steel-concrete composite girder", *J. Constr. Steel Res.*, **159**, 134-146. <https://doi.org/10.1016/j.jcsr.2019.04.031>.
- Esendemir, U. (2006), "The effects of shear on the deflection of simply supported composite beam loaded linearly", *J. Reinf. Plast. Compos.*, **25**(8), 835-846. <https://doi.org/10.1177/0731684406065133>.
- Focacci, F., Foraboschi, P. and Stefano, M.D. (2015), "Composite beam generally connected: analytical model", *Compos. Struct.*, **133**(12), 1237-1248. <https://doi.org/10.1016/j.compstruct.2015.07.044>.
- Foraboschi, P. (2016a), "Effectiveness of novel methods to increase the FRP-masonry bond capacity", *Compos. Part B: Eng.*, **107**(12), 214-232. <https://doi.org/10.1016/j.compositesb.2016.09.060>.
- Foraboschi, P. (2014), "Three-layered plate: Elasticity solution", *Composites Part B: Engineering*, **60**(4), 764-776. <https://doi.org/10.1016/j.compositesb.2013.06.037>.
- Foraboschi, P. (2016b), "Versatility of steel in correcting construction deficiencies and in seismic retrofitting of RC buildings", *J. Build. Eng.*, **8**(12), 107-122. <https://doi.org/10.1016/j.job.2016.10.003>.
- Gao, D.Y. and Zhang, M. (2013), "Calculation method for stiffness of steel fiber reinforced high-strength concrete beams based on effective moment of inertia", *China J. Highway Transport*, **26**(5), 62-68. <https://doi.org/10.19721/j.cnki.1001-7372.2013.05.009>. [In Chinese]
- Girhammar, U.A. (2009), "A simplified analysis method for composite beams with interlayer slip", *Int. J. Mech. Sci.*, **51**(7), 515-530. <https://doi.org/10.1016/j.ijmecsci.2009.05.003>.
- Hanswille, G. and Porsch, M. (2014), "Lifetime oriented design concepts of steel-concrete composite structures subjected to fatigue loading", *Proceedings of the 2008 Composite Construction in Steel and Concrete Conference VI*, Tabernash, CO, USA, July.
- Hanswille, G., Porsch, M. and Ustundag, C. (2007), "Resistance of headed studs subjected to fatigue loading: Part I: Experimental study", *J. Constr. Steel Res.*, **63**(4), 475-484. <https://doi.org/10.1016/j.jcsr.2006.06.035>.
- Hu, S.W. and Zhao, K.Y. (2013), "Experimental research on torsional performance of prestressed composite box beam with partial shear connection", *Appl. Mech. Mater.*, **438-439**, 658-662. <https://doi.org/10.4028/www.scientific.net/AMM.438-439.658>.
- Huang, Y., Wei, J. and Dong, R. (2019), "Stiffness of corroded partially prestressed concrete T-beams under fatigue loading", *Mag. Concr. Res.*, 1-14. <https://doi.org/10.1680/jmacr.18.00187>.
- Kwon, K. and Dan, M.F. (2010), "Bridge fatigue reliability assessment using probability density functions of equivalent stress range based on field monitoring data", *Int. J. Fatigue*, **32**(8), 1221-1232. <https://doi.org/10.1016/j.ijfatigue.2010.01.002>.
- Lin, Z., Liu, Y. and Roeder, C.W. (2016), "Behavior of stud connections between concrete slabs and steel girders under transverse bending moment", *Eng. Struct.*, **117**, 130-144. <https://doi.org/10.1016/j.engstruct.2016.03.014>.
- Liu, F., Zhou, J. and Yan, L. (2018), "Study of stiffness and bearing capacity degradation of reinforced concrete beams under constant-amplitude fatigue", *Plos One*, **13**(3), e0192797. <https://doi.org/10.1371/journal.pone.0192797>.
- Runnian, Y. and Demin, W. (2013), "A study on the residual fatigue strain and damage of steel fiber reinforced recycled concrete under constant amplitude flexural fatigue loading", *J. Test. Eval.*, **41**(3), 465-470. <https://doi.org/10.1520/JTE20120135>.
- Sjaarda, M., Porter, T., West, J.S. and Walbridge, S. (2017),

- “Fatigue behavior of welded shear studs in precast composite beams”, *J. Bridge Eng.*, **22**(11), 04017089. [https://doi.org/10.1061/\(ASCE\)BE.1943-5592.0001134](https://doi.org/10.1061/(ASCE)BE.1943-5592.0001134).
- Song, A., Wan, S., Jiang, Z. and Xu, J. (2018), “Residual deflection analysis in negative moment regions of steel-concrete composite beams under fatigue loading”, *Constr. Build. Mater.*, **158**, 50-60. <https://doi.org/10.1016/j.conbuildmat.2017.09.075>.
- Wang, B., Huang, Q. and Liu, X. (2017), “Deterioration in strength of studs based on two-parameter fatigue failure criterion”, *Steel Compos. Struct.*, **23**(2), 239-250. <https://doi.org/10.12989/scs.2017.23.2.239>.
- Yan, J. B. , Xiong, M.X. , Qian, X. and Liew, J.Y.R. (2016), “Numerical and parametric study of curved steel-concrete-steel sandwich composite beams under concentrated loading”, *Mater. Struct.*, **49**(10), 3981-4001. <https://doi.org/10.1617/s11527-015-0768-2>.
- Yang, T., Lin, G. and Peng, X. (2016), “Experimental study on fatigue behavior of steel-precast concrete slab composite beams with partial shear connection”, *J. Wuhan Univ. Technol.*, **38**(1): 54-58. [in Chinese]
- Yatim, M.Y.M., Shanmugam, N.E. and Badaruzzaman, W.H.W. (2013), “Behaviour of partially connected composite plate girders containing web openings”, *Thin-Wall. Struct.*, **72**(10), 102-112. <https://doi.org/10.1016/j.tws.2013.06.022>.
- Zhou, C., Chen, Z., Shi, S.Q. and Cai, L. (2018), “Behavior of concrete columns confined with both steel angles and spiral hoops under axial compression”, *Steel Compos. Struct.*, **27**(6), 747-759. <https://doi.org/10.12989/scs.2018.27.6.747>.
- Zhou, M., Liu, Z., Zhang, J., An, L. and He, Z. (2016), “Equivalent computational models and deflection calculation methods of box girders with corrugated steel webs”, *Eng. Struct.*, **127**, 615-634. <https://doi.org/10.1016/j.engstruct.2016.08.047>.
- Zhu H., Zhao Y. and Li X. (2014), “Reinforced concrete beam's stiffness degeneration regulation and its calculation formula under the action of fatigue load”, *J. Civil, Architect. Environ. Eng.*, **36**(2):1-13. [In Chinese]